Paleontological Research, vol. 10, no. 1, pp. 91–96, April 30, 2006

Generalized ammonoid hydrostatics modelling, with application to *Intornites* and intraspecific variation in *Amaltheus*

OYVIND HAMMER[1] AND HUGO BUCHER[2]

[1]*Geological Museum, Pb. 1172 Blindern, N-0318 Oslo, Norway (email: ohammer@nhm.uio.no)*

[2]*Paläontologisches Institut und Museum der Universität Zürich, Karl Schmid-Strasse 4, 8006 Zürich, Switzerland*

Received January 7, 2004; Revised manuscript accepted November 17, 2005

Abstract. **A numerical procedure for calculating the buoyancy, apertural orientation and rotational stability of ammonoids can accommodate noncircular apertures and allometries. The hydrostatic properties of the Triassic oxyconic ammonite *Intornites nevadanus* were estimated from measured coiling parameters, body chamber length and digitized whorl section. The calculations indicate close to neutral buoyancy. The orientation of the aperture is 33 degrees from the horizontal, and the stability index relatively high at 0.054. Unlike for many other ammonites, these values are comparable to those of *Nautilus*, suggesting a similar nektobenthic lifestyle. An apertural interior shell callus does not contribute to stability in this genus, and its function remains unknown. In *Amaltheus margaritatus*, hydrostatic properties and body chamber length vary significantly as a result of intraspecific variation in shell shape. Covariation between septal spacing and whorl shape can be given a functional explanation in terms of hydrostatic properties. Buckman's second law of covariation between ribbing and sutural complexity can possibly be thought of in terms of heterochrony.**

Key words: Ammonoids, computer modelling, hydrostatics, intraspecific variation

Introduction

The hydrostatic properties of ammonoids have been investigated by a number of authors, starting with Trueman (1941) who found the centres of buoyancy and gravity using real specimens and plaster casts. Considering the geometric complexity and that material constants are difficult to reproduce in models, many later workers have chosen a computer simulation approach. Raup and Chamberlain (1967) and Chamberlain (1981) calculated and discussed hydrostatic properties in the framework of analytical results for idealized, hypothetical shells in the W/D morphospace. Ebel (1983) used a numerical integration approach for calculating the mass and buoyancy of ammonoids with a range of idealized geometric whorl sections (triangle, trapezoid, etc.). Saunders and Shapiro (1986) used analytical results for shells with circular whorl section to calculate a number of hydrostatic properties of ammonoids placed in the Raup morphospace. Okamoto (1988) used numerical integration to study the orientation of heteromorph ammonoids through ontogeny. Many of these authors assumed that the centre of gravity was equal to the centre of gravity of the body chamber.

Given the decidedly noncircular and nonelliptical whorl section of most ammonoids, and that shell mass probably contributed around ten percent to total mass (see below), these investigations have not addressed the full range of ammonoid morphology with sufficient accuracy. Also, most previous models have not provided the opportunity to estimate centres of gravity and buoyancy of individual parts and materials. We digitized the whorl section of a Triassic oxycone and calculated the hydrostatic properties using a numerical method. This provides the first complete calculation of the centres of buoyancy and gravity of an oxyconic ammonoid.

The method was then used to address a specific problem of ammonoid morphology, namely the observed covariations between whorl shape, coiling parameters, degree of ribbing, complexity of the suture line and interseptal distance.

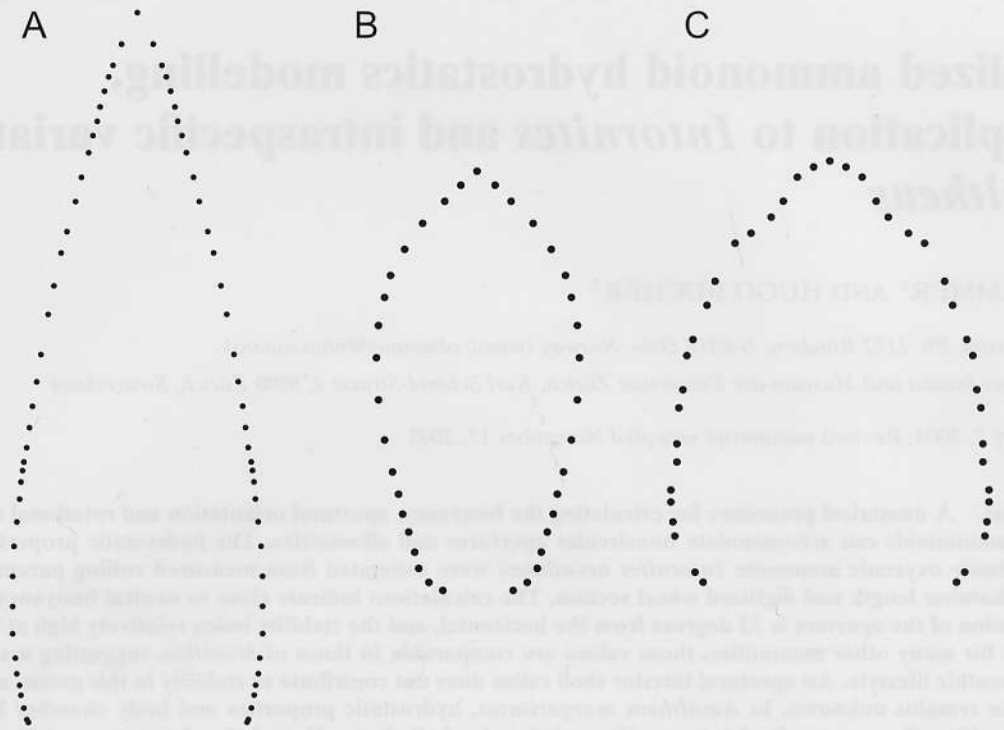

Figure 1. Digitized submature whorl sections of *Intornites* (A), and a compressed and a depressed *Amaltheus* (B and C).

The hydrostatics of *Intornites*

For initial study we chose the Triassic ammonite *Intornites nevadanus*, a typical oxycone with a subtriangular whorl section. The dextral side of a submature whorl section was digitized using the "scan plane" function of a FARO coordinate measuring machine, and the sinistral side produced as its mirror image. A total of 71 points were thus produced along the outline (Figure 1). This outline was then rotated around the coiling axis and expanded into a logarithmic spiral (Figure 2). From measurements on the specimens, we set the whorl expansion rate to $W = 2.76$ (per whorl) and the distance from the coiling axis to $D = 0.01$. We did not include allometry in our model of *Intornites*, under the assumption that most of the hydrostatic properties would be controlled by the shape of the outermost whorls. Also, the ontogenetic change in whorl shape is relatively small in this species. Including allometry would not cause major technical problems for our calculations, however, apart from the dynamic change in whorl overlap, which could be found by a collision detection algorithm.

Again from observations on the specimens, we set the body chamber length to one half whorl (180 degrees). We assumed that the body chamber was entirely filled with soft parts (but see Monks and Young, 1998). Specific weights were chosen according to Saunders and Shapiro (1986), with shell density at 2.62 g/cm^3, soft parts density at 1.055 g/cm^3 and seawater density at 1.026 g/cm^3. It should be noted that contrary to the criticism of Saunders and Shapiro (1986), these values are practically equivalent to those of Ebel (1983), who used values normalized to a sea water density of 1.0. Shell thickness *STH* was allowed to increase linearly with shell diameter d, using a slight adjustment from Ebel (1983) based on observations on *Intornites*: $STH = 0.0050d$.

Septae were also included in the model, although they contribute relatively little to total mass (e.g., Saunders and Shapiro, 1986). We used 20 septae per whorl, each with an area set to half the squared whorl height. This inaccurate approximation is expected to be relatively uncritical for the calculation of hydrostatic properties. Septal thickness *SET* was set to $SET = 0.0025d$ (Ebel, 1983).

Using 1000 steps per whorl over five revolutions, the surface of the shell was constructed from the rotated whorl section, giving a total of 350,000 triangles. Trials with higher numbers of steps did not substantially change the results. Masses and centroids of the triangles were integrated to produce the total mass

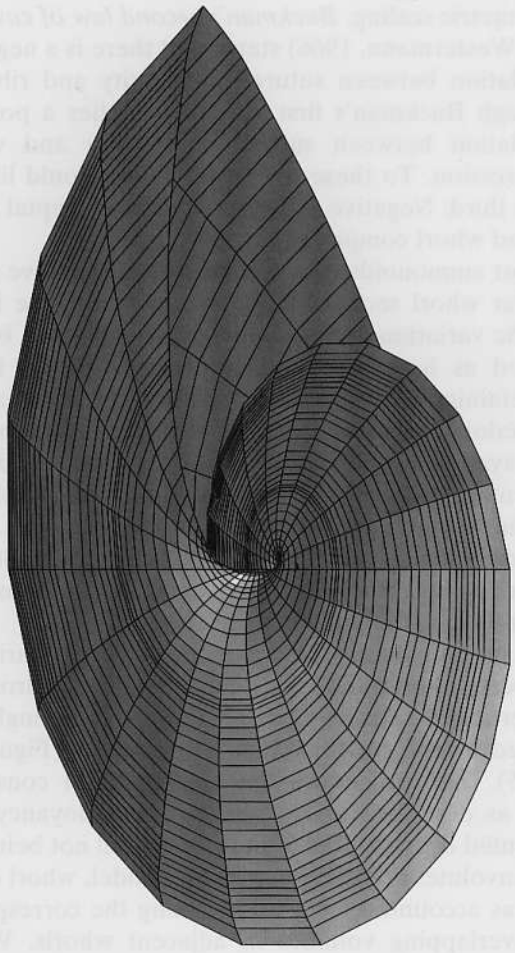

Figure 2. Computer model of *Intornites*, based on the digitized whorl section and measured coiling parameters. For clarity, only 20 elements per whorl are shown.

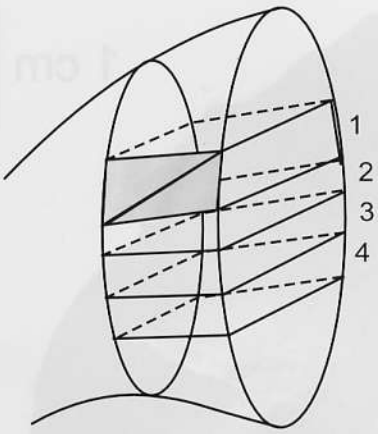

Figure 3. Each segment of the shell between two model steps in the spiral direction is divided into a stack of slices (1–4) in the radial direction, each bounded by two digitized points on the aperture. The lateral shell area on each slice is further divided into triangles, two on each side (only shown on the dextral side of slice 1) for the computation of area and centroid of shell. The internal volume and centroid of each slice are computed by summing the contributions from the two wedge-shaped partitions bounded by the triangles.

and centre of gravity for the outer shell (Figure 3). Septae were similarly included by assuming a centre of gravity at the midpoint between umbilical seam and venter. Total buoyancy and the centre of buoyancy were calculated by integrating the volumes and centroids at each step over the last whorl (the almost complete whorl overlap makes this a valid procedure). The mass and centre of gravity of the soft body were similarly computed by integration through the body chamber, but subtracting the volumes of the penultimate whorl because of whorl overlap.

Like many oxycones, the mature shell of *Intornites* displays a peculiar shell thickening (callus) in the umbilical area just inside the aperture (Figure 4). Inclusion of this feature in the model did not change the hydrostatic properties, due to its small mass (estimated 1.0 g) and its position close to the centre of gravity. This callus can therefore not be explained as an adaptation for increased stability or rotational positioning of the aperture.

The results from the computation are summarized below (coordinate system has the umbilicus as origin, and the final aperture along the positive x axis):

Total shell diameter:	95.18 mm
Mass of outer shell:	9.87 g
Mass of septae:	0.94 g
Total mass (including callus):	59.57 g
Body volume:	45.27 cm^3
Total volume:	57.99 cm^3
Total buoyancy:	59.49 g
Center of gravity (COG):	$x = 9.7$ mm, $y = -15.0$ mm
Center of buoyancy (COB):	$x = 6.8$ mm, $y = -10.7$ mm
COG-COB distance:	5.1 mm
Stability Index:	0.054
Angle between aperture and the horizontal:	33.9 degrees

The total mass is practically identical to total buoyancy, providing neutral buoyancy for this particular ammonoid. Admittedly, this is highly sensitive to values that are perhaps not precisely determined, such as shell thickness and tissue density (Okamoto, 1988).

The Stability Index (COG-COB distance divided by shell diameter) of 0.054 is higher than reported by Sa-

Figure 4. Lateral view of *Intornites*, with most of the body chamber removed. Arrow points to interior shell thickening (callus) close to the aperture of the mature individual.

unders and Shapiro (1986) for ammonites with longer body chambers, ranging from 0.01 to 0.02. However, it is not as high as for *Nautilus* (0.09). The orientation of the aperture is comparable to the 40.94 degrees of *Nautilus* as calculated by Sanders and Shapiro (1986). It can be concluded that the hydrostatic properties of *Intornites* are similar to those of *Nautilus*, but that it is slightly less stable and with a somewhat more upturned aperture.

Intraspecific variation in *Amaltheus*

In *Amaltheus margaritatus*, as in many other ammonoids, there is substantial intraspecific variation in a number of morphological characters (Frentzen, 1937, Howarth, 1958, Meister, 1988). There seems to be considerable structure in this variation, with strong covariation in the characters. Understanding this covariation has taxonomic implications, and can shed light on ammonoid functional and constructional morphology. The so-called *Buckman's first law of covariation* (Westermann, 1966) has two parts: negative correlation between whorl compression and ornamentation, and negative correlation between whorl involution and ornamentation. These observations were explained by Hammer and Bucher (in press) as an effect of isometric scaling. *Buckman's second law of covariation* (Westermann, 1966) states that there is a negative correlation between sutural complexity and ribbing. Through Buckman's first law, this implies a positive correlation between sutural complexity and whorl compression. To these observations we would like to add a third: Negative correlation between septal spacing and whorl compression.

Most ammonoids with compressed shells have more circular whorl sections early in ontogeny. The intraspecific variation in whorl shape can therefore be explained as heterochronic: the more rounded forms are retaining their juvenile shape and can be regarded as paedomorphic. In such forms, where development is delayed, it would not be surprising if sutural development was similarly delayed, retaining the simple suture line of the juvenile into more mature stages. This provides an explanation for Buckman's second law in developmental terms. Other physical mechanisms may also influence the fine shape of the suture.

To investigate the effects of intraspecific variation on apertural orientation, we calculated the hydrostatic properties of a strongly compressed and a strongly depressed morph of *Amaltheus margaritatus* (Figures 1 and 5). The procedure and the material constants were as described above, except that buoyancy was computed over all whorls due to the shell not being totally involute. For each step in the model, whorl overlap was accounted for by subtracting the corresponding overlapping volumes in adjacent whorls. Whorl expansion rates were measured on the specimens and set to $W = 2.92$ for the compressed form, $W = 2.72$ for the depressed form. The ratio between umbilical and ventral radii was set to 0.26 (compressed form) and 0.39 (depressed form). The numbers of septa per whorl were 26 (compressed form) and 18 (depressed form). In the depressed form, the extra shell weight of the ribs was accounted for by a "rib factor" estimated as 1.10.

The body chamber was not preserved in our material. We therefore adjusted the length of the body chamber in the computer model until neutral buoyancy was achieved. This approach was shown by Saunders and Shapiro (1986) to give reasonable results. The compressed form has a higher shell-to-volume ratio than the depressed specimen, and also a larger volumetric ratio between body chamber and phragmocone because of larger whorl expansion rate. Both of these differences reduce buoyancy in the compressed form, which must be compensated for by a shorter body chamber. Consequently, the computed body chamber length is only 0.40 whorls (144 degrees) in the compressed form, compared with a body chamber

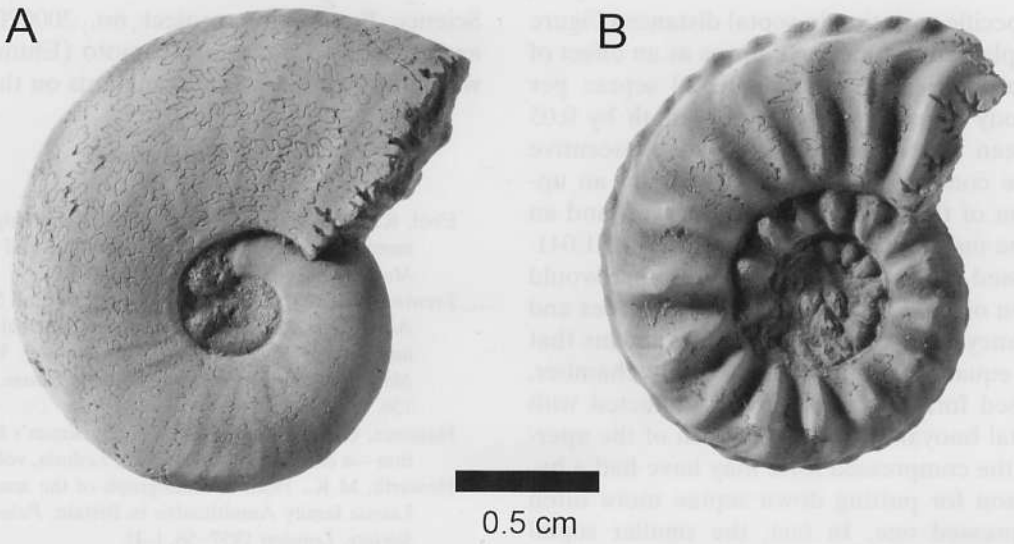

Figure 5. Compressed (A) and depressed (B) morphs of *Amaltheus margaritatus*.

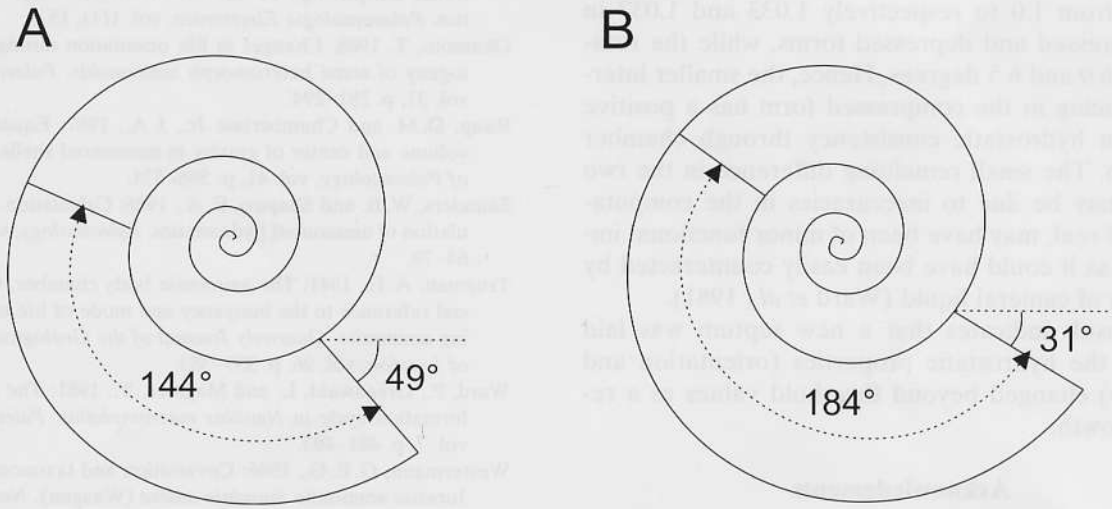

Figure 6. Body chamber length and apertural orientation in the compressed (A) and depressed (B) specimens of *Amaltheus margaritatus*.

length of 0.51 whorls (184 degrees) in the depressed specimen (Figure 6). Apertural orientation (49.1 and 31.0 degrees from the horizontal, respectively) and the stability index (0.057 and 0.049) are also significantly different in the two morphs. The computed body chamber lengths are somewhat smaller than the length of known mature body chambers in *Amaltheus*, which usually slightly exceed one half whorl. Some of the discrepancy may be due to the inaccurate assumption of a planar aperture. Keeping this source of inaccuracy in mind, we can still qualitatively state that the hydrostatic effects of larger whorl width in the depressed than the compressed form is only amplified by differences in whorl expansion rate, and there is no "homeostatic" regulation of several independent parameters to maintain hydrostatic properties across a wide morphological range. However, the stronger ornamentation in the depressed form decreases its buoyancy slightly, bringing it somewhat closer to that of the compressed form.

The intraspecific variation in septal distance (Figure 5) may be explained in functional terms as an effect of hydrostatic properties. If we assume 20 septae per whorl, the body chamber increases in length by 0.05 whorls between the formations of two consecutive septae. In the compressed form, this leads to an upwards rotation of the aperture of 7.6 degrees, and an increase in the mass/buoyancy ratio from 1.0 to 1.041. In the depressed form, the same septal distance would give a rotation of the aperture of only 5.9 degrees and a mass/buoyancy ratio of only 1.034. This means that subjected to equal lengthening of the body chamber, the compressed form is more seriously affected with respect to total buoyancy and orientation of the aperture. Hence, the compressed form may have had a hydrostatic reason for putting down septae more often than the depressed one. In fact, the smaller septal spacing in the compressed form leads to a considerably smaller relative loss of buoyancy and smaller rotation of the aperture between the formations of consecutive septae. The calculated mass/buoyancy ratios increase from 1.0 to respectively 1.033 and 1.037 in the compressed and depressed forms, while the rotations are 6.0 and 6.5 degrees. Hence, the smaller interseptal spacing in the compressed form has a positive impact on hydrostatic consistency through chamber formation. The small remaining difference in the two morphs may be due to inaccuracies in the computation, or, if real, may have been of minor functional importance as it could have been easily counteracted by expulsion of cameral liquid (Ward *et al.*, 1981).

This result indicates that a new septum was laid down as the hydrostatic properties (orientation and buoyancy) changed beyond threshold values as a result of growth.

Acknowledgments

This paper is a contribution to the Swiss National Science Foundation project no. 200020-105090. We are grateful to Takashi Okamoto (Ehime University) who provided important comments on the manuscript.

References

Ebel, K., 1983: Berechnungen zur Schwebefähigkeit von Ammoniten. *Neues Jahrbuch für Geologie und Paläontologie, Monatshefte*, vol. 10, p. 614–640.

Frentzen, K., 1937: Ontogenie, Phylogenie und Systematik der Amaltheen des Lias Delta Südwestdeutschlands. *Abhandlungen der Heidelberger Akademie der Wissenschaften, Mathematisch-naturwissenschaftliche Klasse*, vol. 23, p. 1–136.

Hammer, O. and Bucher, 2005: H. Buckman's law of covariation—a case of proportionality. *Lethaia*, vol. 38, p. 67–72.

Howarth, M. K., 1958: A monograph of the ammonites of the Liassic family Amaltheidae in Britain. *Palaeontographical Society, London* 1957–58, I–II.

Meister, C. 1988: Ontogénèse et evolution des Amaltheidae (Ammonoidea). *Eclogae Geologicae Helvetiae*, vol. 81, p. 763–841.

Monks, N. and Young, J. R., 1998: Body position and the functional morphology of Cretaceous heteromorph ammonites. *Palaeontologia Electronica*, vol. 1(1), 15 p.

Okamoto, T. 1988. Changes in life orientation during the ontogeny of some heteromorph ammonoids. *Palaeontology*, vol. 31, p. 281–294.

Raup, D. M. and Chamberlain Jr., J. A., 1967: Equations for volume and center of gravity in ammonoid shells. *Journal of Paleontology*, vol. 41, p. 566–574.

Saunders, W. B. and Shapiro, E. A., 1986: Calculation and simulation of ammonoid hydrostatics. *Paleobiology*, vol. 12, p. 64–79.

Trueman, A. E., 1941: The ammonite body chamber, with special reference to the buoyancy and mode of life of the living ammonite. *Quarterly Journal of the Geological Society of London*, vol. 96, p. 339–383.

Ward, P., Greenwald, L. and Magnier, Y., 1981: The chamber formation cycle in *Nautilus macromphalus*. *Paleobiology*, vol. 7, p. 481–493.

Westermann, G. E. G., 1966: Covariation and taxonomy of the Jurassic ammonite *Sonninia adicra* (Waagen). *Neues Jahrbuch für Geologie und Paläontologie, Abhandlungen*, vol. 124, p. 289–312.